

Scaling of phytoplankton photosynthesis and cell size in the ocean

Emilio Marañón¹ and Pedro Cermeño

Departamento de Ecología y Biología Animal, Universidad de Vigo, 36210 Vigo, Spain

Jaime Rodríguez

Departamento de Ecología, Universidad de Málaga, 29071 Málaga, Spain

Mikhail V. Zubkov

National Oceanography Centre, University of Southampton, Southampton SO14 3ZH, United Kingdom

Roger P. Harris

Plymouth Marine Laboratory, Prospect Place, Plymouth PL1 3DH, United Kingdom

Abstract

We have determined the scaling relationship between photosynthesis rate and cell size in natural phytoplankton assemblages of contrasting marine environments. We found that phytoplankton photosynthesis in the ocean does not scale as the $\frac{3}{4}$ -power of cell size, but scales approximately isometrically with cell size, indicating that a single model cannot predict the metabolism–size relationship in all photosynthetic organisms. The scaling relationship between cellular chlorophyll *a* content and cell size is also isometric. Taxonomical changes along the size spectrum may explain the deviation of phytoplankton photosynthesis from the general allometric rule. The size scaling exponent for photosynthesis is significantly higher (1.14) in coastal productive waters than in the oligotrophic open ocean (0.96), which provides a physiological basis to explain the dominance of larger cells in nutrient-rich environments. The size scaling exponent for phytoplankton abundance is significantly less negative in coastal productive waters (−0.90) than in the oligotrophic open ocean (−1.25). The observed size scaling relationships imply that carbon fixation per unit volume decreases with cell size in oligotrophic waters, whereas the opposite occurs in productive ones. By controlling the metabolism–size scaling relationship, nutrient supply plays a major role in determining community size structure and the energy flow through the pelagic ecosystem.

The relative importance of small and large phytoplankton is a key feature of the planktonic community, which strongly affects the fate of recently synthesized organic matter in the pelagic ecosystem (Kjørboe 1993; Legendre and Rassoulzadegan 1996; Falkowski et al. 1998). Small cells account for the bulk of phytoplankton biomass in open-ocean oligotrophic waters, where most of the newly produced organic carbon is recycled within the photic layer through complex microbial food webs. By contrast, larger

cells dominate in nutrient-rich productive waters, where a major fraction of primary production is channeled through short food chains and exported toward the ocean interior, thus contributing to CO₂ sequestration. According to the allometric theory in biology (Peters 1983; Brown et al. 2000; Niklas and Enquist 2001), individual metabolic rates (*M*) scale with body size (*V*) as $M \propto V^{3/4}$ (the $\frac{3}{4}$ -power rule or Kleiber's law). A compilation of plant biomass production data covering 20 orders of magnitude in body size, and including laboratory measurements for microalgae, gives support to the view that the $\frac{3}{4}$ -scaling rule applies to all photosynthetic organisms (Niklas and Enquist 2001). If the $\frac{3}{4}$ -power rule holds, it follows that mass-specific metabolism and growth rates must scale as $V^{-1/4}$. This means that smaller cells should dominate all types of pelagic environments, on account of their faster metabolism and growth rates. However, trophic and hydrodynamic mechanisms may also play a role in controlling phytoplankton loss rates and, therefore, their size structure. Thus, the dominance of larger phytoplankton in nutrient-rich areas has been attributed to the stronger grazing pressure suffered by smaller cells (Kjørboe 1993; Irigoien et al. 2005) or to the retention effect of upward water motion (Rodríguez et al. 2001). Nevertheless, this pattern could also arise if higher nutrient availability caused an increase in the size scaling exponent of phytoplankton carbon fixation and growth.

¹ Corresponding author (em@uvigo.es).

Acknowledgments

We thank D. Harbour, F. Jiménez, and L. Zabala for their measurements of phytoplankton abundance and cell size; C. G. Castro and A. J. Bale for nutrient analysis; and B. Mouriño, V. Pérez, and P. Serret for assistance during sampling and the photosynthesis experiments. We also thank X. A. G. Morán, T. Tyrrell, and two anonymous reviewers for their comments on a previous version of the manuscript.

P.C. was supported by a postgraduate research fellowship from the Spanish Ministry of Education and Science (MEC). The research of R.P.H. is a contribution to the Plymouth Marine Laboratory Core Strategic Research Programme. The coastal part of this work was supported by grant REN2000-1248 from the Spanish MEC to E.M. The open ocean part of this work was supported by the U.K. Natural Environmental Research Council through the Atlantic Meridional Transect consortium.

This is contribution 146 of the AMT program.

Abundant evidence suggests that the relationship between cell size of microalgae and their metabolism and growth often deviates from the $3/4$ -power rule (Banse 1982; Chisholm 1992; Finkel 2001), but experimental determinations of the scaling exponent in the relationship between phytoplankton photosynthesis and cell size in the ocean are still lacking. Allometric models have been previously applied to the estimation of phytoplankton productivity in the sea (Joint and Pomroy 1988; Joint 1991; López-Urrutia et al. 2006). These studies combined allometric equations for growth rate (Joint and Pomroy 1988; Joint 1991) and photosynthesis rate (López-Urrutia et al. 2006) with in situ measurements of phytoplankton abundance and cell size to estimate rates of photosynthesis. However, the allometric equations used were based on data from phytoplankton cultures in the laboratory rather than natural assemblages at sea.

Several studies have specifically addressed the experimental determination of the relationship between phytoplankton cell size and photosynthesis in laboratory cultures, typically obtaining scaling exponents around $3/4$ (Blasco et al. 1982; Finkel 2001; Finkel et al. 2004). A limitation of these studies is that they involved a small number of species and covered a modest range in terms of cell size and/or taxonomic variability. In addition, growth conditions in laboratory cultures rarely resemble those encountered by phytoplankton "in situ." Therefore, it is unclear to which extent the size scaling exponents obtained in the laboratory can be extrapolated to natural ecosystems. This has implications for modeling, as most size-based models of plankton structure and metabolic functioning rely on laboratory estimates of the relevant scaling parameters or simply assume the parameters provided by the general allometric theory (Armstrong 1994; López-Urrutia et al. 2006; among others).

The size scaling relationships of individual abundance (N) and M dictate the way in which total energy use per unit area or volume (Q) is partitioned among the differently sized organisms in an ecosystem. Since $Q = N \times M$, if $N \propto V^b$ and $M \propto V^c$, then $Q \propto V^{b+c}$. The energetic equivalence rule states that total energy used by each species is independent of its body size (Damuth 1981). This ecological invariant stems from the common observation that population abundance scales as $V^{-3/4}$ whereas individual metabolic rates scale as $V^{3/4}$ (Damuth 1981; Peters 1983; Brown et al. 2000). In marine phytoplankton, $N \propto V^{-3/4}$ when cell abundance is plotted against mean cell size using pooled data from four biogeographic provinces in the northwestern North Atlantic Ocean (Li 2002). Assuming $M \propto V^{3/4}$, then $Q \propto V^0$, which has led to the suggestion that the amount of energy processed by all phytoplankton in a given size class equals that processed by all phytoplankton in any other size class (Belgrano and Brown 2002). This would indicate that the energy equivalence rule, already validated at the species level in terrestrial plants (Enquist et al. 1998), could be extended to marine phytoplankton when all species within each size class are considered together. However, a specific test of this hypothesis requires the concurrent determination of the size scaling relationships for both N and M .

Table 1. Station location, sampling date, and depths where seawater samples were collected to determine the scaling relationship between cell size, cell abundance, chlorophyll a per cell, and photosynthesis per cell. In the Atlantic Meridional Transect, the stations corresponding to the central gyres are located within the latitudinal ranges 24°N to 35°N and 10°S to 36°S .

Latitude	Longitude	Date	Depths
Ría de Vigo			
$42^\circ14'\text{N}$	$08^\circ47'\text{W}$	05 Sep 2001	Surface, 10 m
$42^\circ14'\text{N}$	$08^\circ47'\text{W}$	11 Apr 2002	Surface, 10 m
$42^\circ14'\text{N}$	$08^\circ47'\text{W}$	15 Apr 2002	Surface, 10 m
$42^\circ14'\text{N}$	$08^\circ47'\text{W}$	18 Apr 2002	Surface, 10 m
$42^\circ14'\text{N}$	$08^\circ47'\text{W}$	22 Apr 2002	Surface, 10 m
$42^\circ14'\text{N}$	$08^\circ47'\text{W}$	30 May 2002	Surface, 10 m
$42^\circ14'\text{N}$	$08^\circ47'\text{W}$	15 Jul 2002	Surface, 10 m
$42^\circ14'\text{N}$	$08^\circ47'\text{W}$	18 Jul 2002	Surface, 10 m
$42^\circ14'\text{N}$	$08^\circ47'\text{W}$	22 Jul 2002	Surface, 10 m
$42^\circ14'\text{N}$	$08^\circ47'\text{W}$	26 Jul 2002	Surface, 10 m
Atlantic meridional transect			
$47^\circ22'\text{N}$	$-18^\circ12'\text{W}$	24 Sep 1996	Surface, 40 m
$42^\circ43'\text{N}$	$-19^\circ48'\text{W}$	25 Sep 1996	Surface, 40 m
$38^\circ10'\text{N}$	$-20^\circ00'\text{W}$	26 Sep 1996	Surface, 40 m
$29^\circ30'\text{N}$	$-21^\circ48'\text{W}$	28 Sep 1996	Surface, 110 m
$24^\circ41'\text{N}$	$-21^\circ24'\text{W}$	29 Sep 1996	Surface, 40 m
$20^\circ04'\text{N}$	$-20^\circ36'\text{W}$	30 Sep 1996	Surface, 20 m, 40 m
$12^\circ46'\text{N}$	$-20^\circ30'\text{W}$	02 Oct 1996	Surface, 20 m
$09^\circ03'\text{N}$	$-22^\circ18'\text{W}$	03 Oct 1996	Surface, 50 m
$05^\circ10'\text{N}$	$-24^\circ00'\text{W}$	04 Oct 1996	Surface, 40 m, 70 m
$01^\circ17'\text{N}$	$-25^\circ48'\text{W}$	05 Oct 1996	Surface, 40 m, 80 m
$02^\circ23'\text{S}$	$-27^\circ30'\text{W}$	06 Oct 1996	Surface, 40 m, 85 m
$06^\circ29'\text{S}$	$-29^\circ18'\text{W}$	07 Oct 1996	Surface, 50 m, 110 m
$10^\circ47'\text{S}$	$-31^\circ12'\text{W}$	08 Oct 1996	Surface, 75 m, 130 m
$15^\circ13'\text{S}$	$-32^\circ48'\text{W}$	09 Oct 1996	Surface, 60 m, 140 m
$18^\circ52'\text{S}$	$-35^\circ01'\text{W}$	10 Oct 1996	Surface, 75 m, 125 m
$22^\circ56'\text{S}$	$-37^\circ00'\text{W}$	11 Oct 1996	Surface, 60 m, 100 m
$26^\circ37'\text{S}$	$-39^\circ36'\text{W}$	12 Oct 1996	Surface, 95 m
$29^\circ51'\text{S}$	$-42^\circ54'\text{W}$	13 Oct 1996	Surface, 50 m, 90 m
$32^\circ48'\text{S}$	$-46^\circ06'\text{W}$	14 Oct 1996	Surface, 40 m, 60 m
$35^\circ43'\text{S}$	$-49^\circ36'\text{W}$	15 Oct 1996	Surface, 30 m, 50 m
$37^\circ49'\text{S}$	$-52^\circ12'\text{W}$	22 Oct 1996	Surface, 40 m, 60 m
$43^\circ35'\text{S}$	$-55^\circ00'\text{W}$	23 Oct 1996	Surface, 30 m, 50 m
$48^\circ00'\text{S}$	$-55^\circ54'\text{W}$	24 Oct 1996	Surface, 40 m

Here we present the first determinations of the size scaling exponent for phytoplankton photosynthesis in the ocean, with the aim of testing the hypothesis that phytoplankton metabolism follows the general $3/4$ -power rule. Our observations in contrasting marine environments serve to determine the effect of nutrient supply on the size scaling of photosynthesis and the size structure of the phytoplankton community. Finally, we analyze the size scaling of phytoplankton abundance, which enables us to assess how energy use by photosynthesis changes along the size spectrum in productive versus unproductive ecosystems.

Methods

Sampling—To determine the size scaling relationships for phytoplankton abundance, chlorophyll a (Chl a) cell

content, and photosynthesis per cell, we measured ^{14}C -uptake, Chl *a* concentration, cell volume, and cell abundance across the entire range of phytoplankton cell size, including picophytoplankton ($0.2\text{--}2\ \mu\text{m}$), nanophytoplankton ($2\text{--}20\ \mu\text{m}$), and microphytoplankton ($>20\ \mu\text{m}$). Samples were taken in a central station of the highly productive Ría de Vigo (NW Spain) during the upwelling season (April to September 2002) (Cermeño et al. 2005b) and in the open ocean during an Atlantic Meridional Transect ([AMT] October 1996) (Marañón et al. 2000; Marañón et al. 2001) (see Table 1 for station location and sampling dates). In total, we performed 20 experiments in the Ría de Vigo and 60 experiments during the AMT (Table 1). The AMT covers $\sim 13,000\ \text{km}$ from 50°N to 50°S and crosses temperate, subtropical, tropical, and equatorial regions. In the Ría de Vigo survey, water samples were collected from the surface and from 10-m depth, which corresponded approximately to the 20% light extinction level. In the AMT survey, samples were typically collected at the surface and near the 20% and 1% light extinction levels (Table 1). The combined data set spans approximately six orders of magnitude in cell-specific photosynthesis rates, cell volume, and cell abundance.

Photosynthesis—Size-fractionated photosynthesis was determined with the ^{14}C -uptake technique during short (2–6 h), on-deck incubations (Marañón et al. 2001; Cermeño et al. 2005b). Using clean techniques and taking particular care to avoid any light shock to the phytoplankton populations, water samples were collected and transferred to 80-mL, acid-washed polycarbonate bottles to which 370–740 KBq of $\text{NaH}^{14}\text{CO}_3$ were added. Samples (three light bottles and one dark bottle) were incubated at their original irradiance level, which was simulated by using a combination of blue (Mist Blue, Lee Filters No. 061) and neutral density filters. Temperature was kept constant by means of running water that was pumped from the surface (in the AMT cruise) or circulated through refrigerators (in the Ría de Vigo cruises). After incubation, samples were sequentially filtered, using low-vacuum pressure ($<13.5\ \text{kPa}$), through polycarbonate filters of $20\ \mu\text{m}$, $2\ \mu\text{m}$, and $0.2\ \mu\text{m}$ in pore size. In the Ría de Vigo cruises, the use of an additional filter enabled us to distinguish photosynthesis by small ($2\text{--}5\ \mu\text{m}$) and large ($5\text{--}20\ \mu\text{m}$) nanophytoplankton (Cermeño et al. 2005b). The comparison with parallel experiments in which total photosynthesis was measured in non-fractionated samples revealed that sequential filtration does not have any effect on the resulting estimates of carbon fixation. Dark-bottle ^{14}C activity was subtracted from the light-bottle ^{14}C activity. The mean coefficient of variation in the photosynthesis measurements was 13% for the AMT samples and 9% for the Ría de Vigo samples.

If grazing by protists is important during the ^{14}C uptake experiments and affects small and large cells differently, then the resulting photosynthesis–size relationship may be biased. However, the short incubation times used imply that ^{14}C losses due to grazing were likely to be small in our experiments. It must be noted that for grazing to represent

a loss of fixed ^{14}C , and thus lead to an underestimation of productivity, ingested ^{14}C must be either excreted or respired. We used the model of Laws (1984) to constrain the degree to which grazing may have caused an underestimation of phytoplankton production in the experiments. Assuming the worst-case scenario of high phytoplankton growth rates ($1\ \text{d}^{-1}$ in the central gyres and $2\ \text{d}^{-1}$ in the Ría de Vigo), heavy grazing pressure (grazing rate equal to 99% of phytoplankton growth rate), and low growth efficiency of grazers (70% of ingested ^{14}C is respired or excreted), grazing may have reduced phytoplankton production by a factor of up to 8% and 5% in the central gyres and the Ría de Vigo, respectively. These low figures indicate that our estimates of phytoplankton photosynthesis and the resulting size–photosynthesis relationships were not significantly affected by grazing during the ^{14}C uptake experiments.

Chl *a*, cell size, and abundance—Chl *a* concentration was measured fluorometrically on the same size classes as photosynthesis after sequential filtration of duplicate 250-mL samples through polycarbonate filters and subsequent extraction in 90% acetone (Marañón et al. 2001; Cermeño et al. 2005b). Phytoplankton cell volume and abundance were measured by combining two techniques: flow cytometry for picophytoplankton and small nanophytoplankton (Rodríguez et al. 1998; Zubkov et al. 1998; Cermeño et al. 2005b), and optical microscopy for large nanophytoplankton and microphytoplankton (Rodríguez et al. 1998; Marañón et al. 2000; Rodríguez et al. 2001). For flow cytometry, water samples of 2–10 mL in volume were preserved with 1% (v/v) glutaraldehyde and stored in liquid nitrogen until analysis with a FACScan (Ría de Vigo samples) or a FACSsort (AMT samples) flow cytometer (Becton Dickinson). In the case of the Ría de Vigo samples, the size and abundance of all cells in the range $0.6\text{--}10\ \mu\text{m}$ of equivalent spherical diameter (ESD) were determined by using their fluorescence and side light scatter (SLS) signals. The latter were calibrated with image-analysis measurements of the volume of several species cultured in the laboratory, which enabled us to compute the size of each cell (Rodríguez et al. 1998). In the case of the AMT samples, the SLS and fluorescence signals were used to identify and count the cells belonging to the three main groups of autotrophic picophytoplankton (*Prochlorococcus*, *Synechococcus*, and picoeukaryotes) (Zubkov et al. 1998). The mean cell size of *Prochlorococcus* and *Synechococcus* was determined by size fractionation through multiple filters of different pore sizes and subsequent counting of the intact sample and each filtrate. The mean cell volume of picoeukaryotes was determined by image analysis on an epifluorescence microscope (Zubkov et al. 1998). Finally, the cell volume and abundance of nanophytoplankton and microphytoplankton were measured following Utermöhl's method. One hundredmilliliter samples were preserved in 1% buffered formalin, and after sedimentation of a sub-sample (10–20 mL for Ría de Vigo samples, 50–100 mL for AMT samples) cells were counted and measured on an inverted microscope. Individual linear measurements were used to compute cell volume by

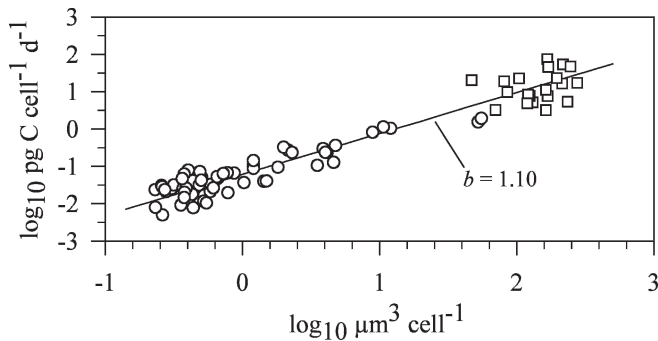


Fig. 1. Across-systems photosynthesis–cell size relationship. Total cell-specific photosynthesis is plotted against mean cell volume of the phytoplankton assemblage. Samples were obtained along a meridional transect in the open Atlantic Ocean from 50°N to 50°S (circles, 60 samples) and in a coastal, productive ecosystem (Ría de Vigo, NW Spain) (squares, 20 samples). The reduced major axis regression line is: $\log_{10} [y] = -1.21 + 1.10 \log_{10} [x]$ ($r^2 = 0.93$, $p < 0.001$, $n = 80$, 95% CI for $b = 1.02$, 1.16).

assigning each cell to the geometric shape that most closely resembled the real shape of each species.

Data analysis—Using data from the entire AMT cruise (50°N to 50°S) (60 experiments) and the Ría de Vigo during the upwelling season (20 experiments), we divided total photosynthesis by total number of phytoplankton cells in each sample. The resulting rates of cell-specific photosynthesis were plotted against the abundance-weighted, mean cell volume of the whole phytoplankton assemblage, thus yielding an across-systems scaling relationship between photosynthesis and cell size (Fig. 1). This approach is analogous to that used by Li (2002), who studied the relationship between total cell abundance and the average cell size of the phytoplankton assemblages. Although this approach is useful to identify overall macroecological patterns across different ecosystems, the use of mean assemblage cell size may distort the resulting size scaling relationships. For instance, if environmental conditions, such as temperature or resource supply, change along the geographical gradient considered, the resulting slope in the overall size scaling relationship may be affected by the existence of grade shifts between groups of data, which may have similar slopes but different intercepts.

To circumvent these problems, we also determined the scaling relationship between cell size and photosynthesis at the local scale for each particular phytoplankton assemblage present on each sample. We used our measurements of size-fractionated photosynthesis to construct these local size scaling relationships. Using our data of phytoplankton cell size and abundance, we first determined total cell abundance and the abundance-weighted mean cell volume for each size class. Cells were assigned to a particular size class according to their ESD. We then divided the measured photosynthesis rate on each size class by the number of cells present in that particular size class. Finally, cell-specific photosynthesis in each size class was plotted against the mean cell volume of the size class, and the procedure was repeated for each sample to construct plots

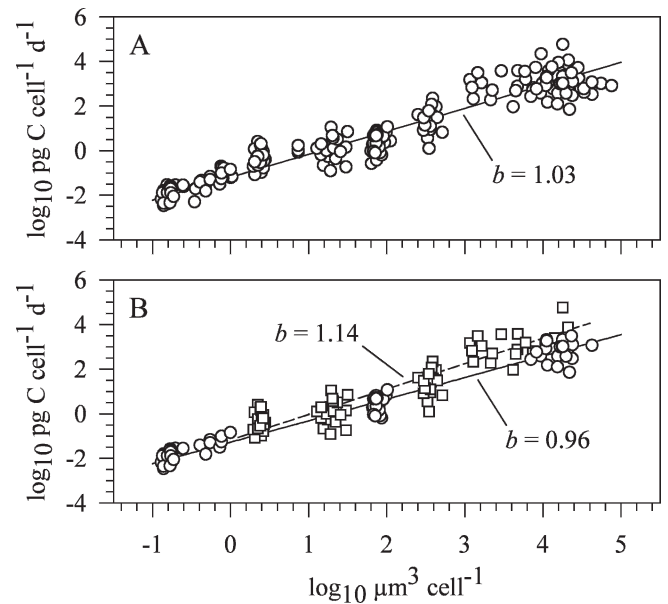


Fig. 2. Photosynthesis–cell size relationships in size-fractionated phytoplankton. Cell-specific photosynthesis in each phytoplankton size class is plotted against the mean cell volume of the size class. (A) All data from Ría de Vigo and the Atlantic Ocean (50°N to 50°S). (B) Data from the North and South Atlantic central gyres (circles, solid line) and the Ría de Vigo (squares, dashed line). See Table 2 for statistics.

such as those shown on Fig. 2. A limitation of this procedure, however, is that it considers only a small number of discrete size classes (three or four), reflecting the number of size fractions where photosynthesis was determined. Ideally, one would like to know the cell-specific photosynthetic rate of each phytoplankton species present in the assemblage. This, however, is not possible with currently available methods.

In order to verify if our discrete approach yields reliable estimates of the slope and intercept of the logarithmic relationship between metabolic rate and cell size, consider an idealized assemblage of phytoplankton species with theoretically given size scaling parameters for both abundance and photosynthesis rate. The assemblage is composed of >80 species with cell size ranging between $0.15 \mu\text{m}^3$ and $5.2 \times 10^5 \mu\text{m}^3$. The cell sizes of the different species do not overlap, so that species are distributed along the size spectrum in such a way that each size interval of $0.25 \log_2$ cell volume (V , μm^3) in width contains one single species. The abundance of each species is given by aV^b , where a takes an arbitrary value of $10^4 \text{ cell mL}^{-1}$ and b can take any set value between -1.4 and -0.8 . Similarly, the cell-specific photosynthetic rate for each species is given by $a'V^{b'}$, where a' takes an arbitrary value of $0.03 \text{ pg C cell}^{-1} \text{ d}^{-1}$ and b' can take any set value between 0.7 and 1.2 . The choice of values for the coefficients a and a' is irrelevant for our argument. The photosynthesis by each species is calculated by multiplying its abundance by its cell-specific photosynthetic rate. One can then calculate total cell abundance and total photosynthesis in any given size range, simply by summing the abundance and photosyn-

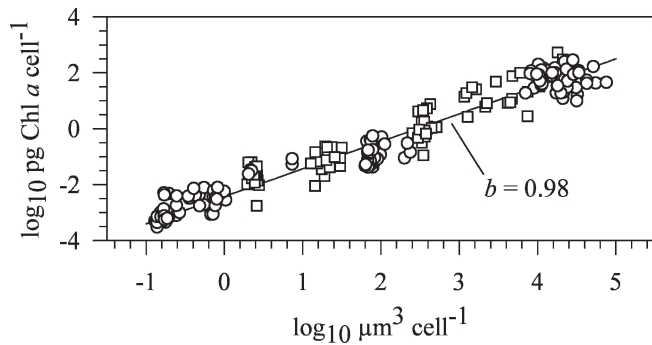


Fig. 3. Chl *a*-cell size relationship in size-fractionated phytoplankton. Cell-specific Chl *a* concentration in each phytoplankton size class is plotted against the mean cell volume of the size class. Data are from the AMT (50°N to 50°S, circles) and the Ría de Vigo (squares). The reduced major axis regression line is: $\log_{10} [y] = -2.42 + 0.98 \log_{10} [x]$ ($r^2 = 0.94$, $p < 0.001$, $n = 254$, 95% CI for $b = 0.95, 1.01$).

thesis of all species whose ESD falls within that particular size range. The mean cell size of the ensemble of all species within a given size range can also be computed. Finally, dividing photosynthesis by cell abundance gives cell-specific photosynthesis in each size class considered. In this way, we determined the linear relationship between \log_{10} cell volume and \log_{10} photosynthesis per cell using three or four data points, corresponding to the size classes considered (e.g., 0.2–2 μm , 2–20 μm , and >20 μm or 0.2–2 μm , 2–5 μm , 5–20 μm , and >20 μm in cell diameter). We found that for a range of values of the size scaling exponents for cell abundance ($-1.4 < b < -0.8$) and cell-specific photosynthesis ($0.7 < b' < 1.2$) the parameters of the scaling relationship between \log_{10} photosynthesis and \log_{10} cell volume, as estimated by the discrete approach, were virtually identical to the expected values. The calculated values differed from the theoretically given values by <1% in the case of the scaling exponent and <4% in the case of the intercept. The same results were obtained when the procedure was applied to real abundance-size spectra obtained in the Ría de Vigo and in the Atlantic subtropical gyres. We thus conclude that our method to determine the relationship between cell size and photosynthesis based on the use of size-fractionated photosynthesis data yields reliable estimates of the relevant scaling parameters.

Chl *a* content per cell was calculated by dividing the Chl *a* concentration on each size fraction by the number of cells within that size fraction (Fig. 3). Abundance-size relationships were constructed by distributing the abundance data along an octave (\log_2) scale of cell volume (Rodríguez et al. 1998). The abundance of all cells within each size interval was summed, and the resulting abundance was plotted against the nominal size of the interval (Fig. 4). Reduced major-axis regression was applied to \log_{10} -transformed variables to determine the parameters of the size scaling relationship. The slope of the linear regression represents the size scaling exponent in the power equation relating abundance or photosynthesis to cell volume. Ninety-five percent confidence intervals (CIs) for the regression

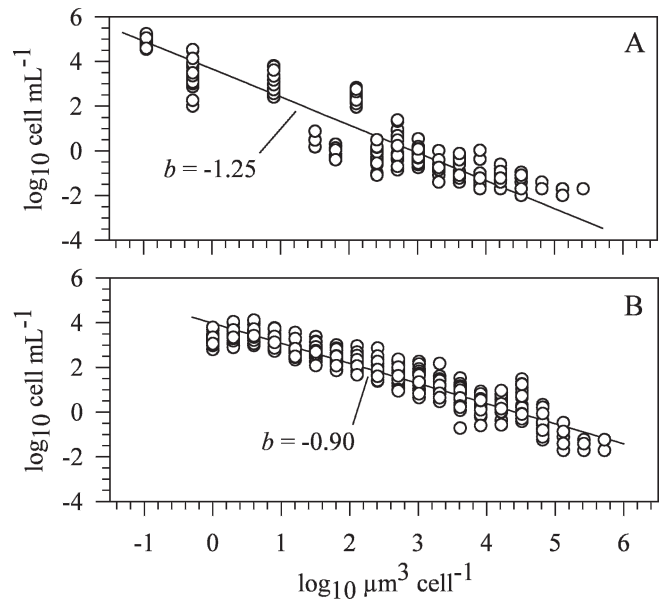


Fig. 4. Abundance-cell size relationships. Total cell abundance in each size interval is plotted against the nominal cell volume of the interval. Data are from (A) the North and South Atlantic central gyres and (B) the Ría de Vigo. See Table 2 for statistics.

parameters were calculated by bootstrapping over cases (2,000 repetitions).

Results and discussion

The across-systems analysis of all data from the open Atlantic Ocean (50°N–50°S) and the Ría de Vigo showed that assemblage mean cell volume is a good predictor ($r^2 = 0.93$, $p < 0.001$) of total, cell-specific photosynthesis, despite large changes in environmental conditions and phytoplankton taxonomic composition along the size spectrum (Fig. 1). The scaling exponent (1.10) was significantly higher (two-tailed *t*-test, $p < 0.001$) than 0.75, the value commonly reported for the allometric scaling of metabolism in plants and animals (Peters 1983; Niklas and Enquist 1999; Brown et al. 2000), suggesting that phytoplankton photosynthesis in natural ecosystems does not follow the $3/4$ -power rule. However, the across-system relationship shown on Fig. 1 cannot be interpreted in terms of the effect of cell size alone, because the different assemblages across the size spectrum were also experiencing widely differing temperature and nutrient conditions, which may affect the photosynthesis-size relationship.

In order to isolate the effect of cell size and determine the photosynthesis-size relationship over a wider size range, we plotted together all measurements of cell-specific photosynthesis and mean cell volume in size-fractionated phytoplankton obtained along the AMT and in the Ría de Vigo. Data from all sampled depths were plotted together because our objective was to define a general macroecological pattern in the relationship between cell size and photosynthesis rather than analyze its variability at the local scale. For the entire data set, the relationship between photosynthesis and cell size was approximately

Table 2. Parameters of the size scaling relationships for phytoplankton photosynthesis and abundance in the Atlantic Meridional Transect (AMT) and the Ría de Vigo surveys. The AMT stations corresponding to the central gyres are located within the latitudinal ranges 24°N to 35°N and 10°S to 36°S. Reduced major axis regression was used to determine the relationship between \log_{10} phytoplankton cell volume ($\mu\text{m}^3 \text{ cell}^{-1}$) (independent variable) and \log_{10} photosynthesis per cell ($\text{pg C cell}^{-1} \text{ d}^{-1}$) and \log_{10} phytoplankton abundance (cell mL^{-1}) (dependent variables). Bootstrap confidence limits (95%) for the intercept (a) and the slope (b) are given in parentheses. In all regressions, $p < 0.001$. The last column indicates the figure and panel where each particular data set is represented. DCM indicates samples from the deep chlorophyll a maximum.

Dataset	a	b	r^2	n	Fig.
Photosynthesis					
AMT + Ría de Vigo, all depths	-1.19 (-1.27, -1.11)	1.03 (0.99, 1.07)	0.91	234	2A
Central gyres, all depths	-1.27 (-1.34, -1.17)	0.96 (0.92, 0.99)	0.97	76	2B
Central gyres, surface samples	-1.21 (-1.24, -1.07)	0.99 (0.93, 1.02)	0.99	28	
Central gyres, DCM samples	-1.16 (-1.32, -1.05)	0.92 (0.85, 0.98)	0.96	30	
Ría de Vigo, all depths	-1.16 (-1.41, -0.92)	1.14 (1.03, 1.24)	0.83	79	2B
Ría de Vigo, surface samples	-1.51 (-1.80, -1.05)	1.22 (1.03, 1.36)	0.81	40	
Ría de Vigo, 10 m samples	-0.98 (-1.21, -0.66)	1.10 (0.94, 1.21)	0.90	39	
Abundance					
Central gyres, all depths	3.66 (3.51, 3.82)	-1.25 (-1.29, -1.21)	0.86	262	4A
Central gyres, surface samples	3.74 (3.52, 3.97)	-1.25 (-1.32, -1.18)	0.88	98	
Central gyres, DCM samples	3.48 (3.23, 3.71)	-1.21 (-1.28, -1.14)	0.83	106	
Ría de Vigo, all depths	3.98 (3.89, 4.08)	-0.90 (-0.93, -0.86)	0.89	356	4B
Ría de Vigo, surface samples	4.20 (4.03, 4.31)	-0.94 (-0.98, -0.88)	0.93	176	
Ría de Vigo, 10-m samples	3.83 (3.74, 3.93)	-0.87 (-0.91, -0.82)	0.94	180	

isometric (Fig. 2A), thus confirming that phytoplankton photosynthesis does not follow the $3/4$ -power rule. The value of the slope (1.03) was again significantly higher than 0.75 (two-tailed t -test, $p < 0.001$). This finding was supported by the observation of an isometric relationship between cell volume and intracellular Chl a content (which is a proxy for phytoplankton biomass and photosynthetic capacity) (Fig. 3) and, accordingly, between cell-specific photosynthesis and Chl a per cell (data not shown). The isometric scaling between cell volume and intracellular Chl a contrasts with previous observations of phytoplankton in laboratory cultures, which typically indicate a size scaling exponent in the range 0.6–0.8 (see Finkel et al. 2004 and references therein). These differences may reflect the widely different growth conditions experienced by laboratory cultures and natural phytoplankton and the fact that most laboratory studies are carried out with just a small number of species within a few divisions (typically, diatoms, haptophytes, and chlorophytes), whereas natural phytoplankton assemblages are composed by numerous species belonging to many different taxonomic groups. Together with a recent report of isometric scaling between individual respiration and mass in higher plants (Reich et al. 2006), our results show that a single, universal scaling rule (Enquist et al. 1998; Niklas and Enquist 2001) cannot predict the metabolism–size relationship in all photosynthetic organisms.

Our observations suggest little size dependence of phytoplankton growth rate and size-specific metabolism in natural conditions. In their studies on the application of allometric methods to estimate phytoplankton productivity in the sea, Joint and Pomroy (1988) and Joint (1991) also concluded that a less negative size scaling exponent for growth rate (e.g., -0.15 instead of -0.25, implying a smaller size dependence of growth) gave a better description of in situ phytoplankton productivity. Similar

conclusions were attained by Sommer (1989), who found that the size scaling exponent for the maximum growth rate of Antarctic phytoplankton was -0.066. In contrast, a recent study by López-Urrutia et al. (2006), who compiled an extensive data set of phytoplankton cell size, production, and growth in laboratory cultures, supports the view that phytoplankton photosynthesis follows the $3/4$ -scaling rule. These contrasting results suggest that there may be fundamental differences between the size scaling of phytoplankton metabolism in laboratory cultures and that of natural assemblages at sea.

Although macroecological studies emphasize the search for common patterns across communities and ecosystems (Enquist et al. 1998; Brown et al. 2000; Li 2002), we also analyzed the photosynthesis–size relationship separately in the central Atlantic gyres (stations located in the latitudinal ranges 24°N to 35°N and 10°S to 36°S, see Table 1) and in the Ría de Vigo, because these two ecosystem types are widely contrasting in terms of environmental forcing, phytoplankton size structure, and biogeochemical functioning (Marañón et al. 2000; Marañón et al. 2001; Cermeño et al. 2005b). This approach enabled us to test the effects of nutrient availability on the scaling between metabolism and cell size (Finkel 2001; Finkel et al. 2004; Reich et al. 2005). Mean nitrate and Chl a concentrations at the surface were $1.3 \mu\text{mol L}^{-1}$ and 4.7 mg m^{-3} , respectively, in the Ría de Vigo (Cermeño et al. 2005b), as compared to $0.05 \mu\text{mol L}^{-1}$ and 0.16 mg m^{-3} in the central Atlantic gyres (Marañón et al. 2000). The relative contribution of $>20\text{-}\mu\text{m}$ phytoplankton to total biomass and production was $>90\%$ in the Ría de Vigo (Cermeño et al. 2005a,b) and $<10\%$ in the central Atlantic gyres (Marañón et al. 2001).

The slope of the photosynthesis–size relationship was significantly lower in the oligotrophic Atlantic central gyres

($b = 0.96$, 95% CI = 0.92–0.99) than in the productive Ría de Vigo ($b = 1.14$, 95% CI = 1.03–1.24) (Fig. 2B). On Fig. 2B, data from all sampled depths are plotted together. When we analyzed separately the data from surface and deep samples, we found that within each ecosystem type there were no significant differences in the regression parameters between depths, although the slope of the photosynthesis–size relationship tended to be somewhat higher in the surface samples (Table 2). High values of the photosynthesis size scaling exponent occurred in surface and deep samples of both ecosystems, and for a given depth level the slopes in the Ría de Vigo were always significantly higher than those measured in the subtropical gyres (Table 2). The significance of the high slopes measured in the eutrophic waters of the Ría de Vigo can be illustrated as follows. Assuming cell carbon (C) scales isometrically with cell volume ($C \propto V^1$), a size scaling exponent for photosynthesis of 1.14 implies that a typical microphytoplankton cell ($V \sim 14,000 \mu\text{m}^3$, ESD $\sim 30 \mu\text{m}$) will have a C turnover rate approximately four and two times faster than a typical cell of picophytoplankton ($V \sim 1.4 \mu\text{m}^3$, ESD $\sim 1.4 \mu\text{m}$) and nanophytoplankton ($V \sim 400 \mu\text{m}^3$, ESD $\sim 9 \mu\text{m}$), respectively. These differences would be even more dramatic if, as frequently reported for laboratory cultures, cell C scales to cell V with an exponent lower than one. Thus, the dominance by larger phytoplankton in nutrient-rich waters does not necessarily reflect an indirect trophic mechanism (e.g., the different grazing pressure suffered by small and large cells [Kjørboe 1993; Irigoien et al. 2005]), but may result from a direct physiological response; namely, an increase in the size scaling exponent of carbon fixation, which means that under high-resource conditions larger algae grow faster than smaller photoautotrophs.

On theoretical grounds, biomass-specific resource acquisition and growth rates should decrease with increasing cell size as the surface to volume ratio gets smaller and the pigment package effect is enhanced (Chisholm 1992; Kjørboe 1993; Raven 1998). However, the conspicuously high value of the size scaling exponent for photosynthesis suggest that other factors, in addition to geometrical constraints on resource acquisition and use, must be considered to explain the metabolism–size relationship of phytoplankton in natural ecosystems. Specifically, changes in taxonomic composition along the size spectrum are likely to be of major significance. Larger phytoplankton, and diatoms in particular, possess several strategies that may override the effects of cell size per se. They include the increase in the effective surface to volume ratio due to changes in cell shape and the presence of the vacuole, the accumulation of non-limiting substrates to increase size and optimize nutrient uptake (Thingstad et al. 2005), and the ability to sustain high specific uptake rates and store large amounts of nutrients under conditions of discontinuous supply (Stolte et al. 1994). These factors may explain a growing body of evidence indicating that, in natural conditions at sea, larger algae frequently attain higher photosynthetic efficiencies (Cermeño et al. 2005a; Claustre et al. 2005) and faster growth rates (Latasa et al. 2005) than picophytoplankton and small nanophytoplankton. The

high value of the size scaling exponent for photosynthesis has major biogeochemical implications, because larger phytoplankton are responsible for most of the exported primary production in the ocean (Legendre and Rassoulzadegan 1996; Falkowski et al. 1998).

The concurrent analysis of the size scaling relationships for phytoplankton abundance and cell-specific photosynthesis enables the prediction of how total carbon fixation per unit volume (Q) changes along the size spectrum. In the Atlantic central gyres, when all samples from the various sampling depths were pooled together, the slope of the phytoplankton size–abundance relationship was -1.25 (Fig. 4A). We did not find statistically significant differences in the parameters of the size–abundance relationship between surface and deep samples, although the intercept tended to take higher values in surface samples (Table 2). The steep slope of the size–abundance relationships in the central gyres reflects the marked dominance by small cells and coincides with values previously found in the oligotrophic open ocean (typically in the range -1.0 to -1.4) (Cavender-Bares et al. 2001). The size–abundance relationships presented here (Fig. 4) are constructed by plotting the total abundance of all species within each size class against the nominal size of that class (*see* Methods). They should not be confused with the relationship between population abundance and cell size, in which each data point represents a single species. In a recent analysis, we showed that the population abundance of marine phytoplankton scales invariantly as the $-3/4$ -power of cell volume, regardless of environmental conditions (Cermeño et al. 2006). The fact that in the subtropical gyres total abundance scales with cell size with a unequivocally more negative slope than in coastal waters (Fig. 4) points to significant differences in the relationship between cell size and species richness in contrasting marine environments.

Compared with the subtropical gyres, the Ría de Vigo showed size–abundance relationships with a less negative slope (-0.90 ; Fig. 4B), indicative of an increase in the relative contribution of larger cells to total cell abundance. There were no significant differences in the size scaling of abundance between surface and deep samples in the Ría de Vigo, although the surface data subset showed higher intercept values (Table 2). Similar slopes (in the range -0.90 to -0.70) have been reported before for coastal, productive waters (Reul et al. 2005). The slope of the size–abundance relationship in nutrient-rich waters reinforces the view that the size scaling exponent for phytoplankton photosynthesis is likely to be higher than $3/4$; if it were not, total photosynthesis per unit volume would scale with cell size with an exponent ≤ 0 , in clear contradiction with the well established dominance of large phytoplankton in productive ecosystems (Chisholm 1992). Thus, in the Atlantic central gyres $Q \propto V^{-1.25} \times V^{0.96} = V^{-0.29}$, whereas in the Ría de Vigo $Q \propto V^{-0.90} \times V^{1.14} = V^{0.24}$, which means that total energy processed by phytoplankton photosynthesis decreases with cell size in open-ocean oligotrophic waters, whereas it increases in nutrient-rich productive waters. Consequently, and contrary to the suggestion made by Belgrano and Brown (2002), the energetic equivalence rule does not hold for marine

phytoplankton at the species assemblage level, in agreement with available evidence on the partitioning of primary productivity among different size classes and the potential for biogenic carbon export in contrasting marine environments (Chisholm 1992; Legendre and Rassoulzadegan 1996).

In summary, we have shown that the scaling of phytoplankton photosynthesis and cell size deviates significantly from the $3/4$ -power rule and, additionally, that it is not constant but depends on nutrient availability. A high ($>3/4$) and variable size scaling exponent for phytoplankton photosynthesis is the only way to reconcile phytoplankton size–abundance relationships (Rodríguez et al. 2001; Cavender-Bares et al. 2001; Reul et al. 2005) with the partitioning of carbon fixation among different size classes in productive and unproductive marine ecosystems (Chisholm 1992; Marañón et al. 2001). It also suggests that trophic processes do not need to be invoked to explain the dominance of larger phytoplankton in nutrient-rich waters. Our results question the universality of the $3/4$ -power rule for photoautotrophic biomass production (Niklas and Enquist 2001) and highlight the role of resource supply (Finkel 2001; Finkel 2004) in controlling the metabolism–size scaling relationship and thus community size structure and energy flow through the ecosystem.

References

- ARMSTRONG, R. A. 1994. Grazing limitation and nutrient limitation in marine ecosystems: Steady state solutions of an ecosystem model with multiple food chains. *Limnol. Oceanogr.* **39**: 597–608.
- BANSE, K. 1982. Cell volumes, maximal growth rates of unicellular algae and ciliates, and the role of ciliates in the marine pelagial. *Limnol. Oceanogr.* **27**: 1059–1071.
- BELGRANO, A., AND J. H. BROWN. 2002. Oceans under the microscope. *Nature* **419**: 128–129.
- BLASCO, D., T. T. PACKARD, AND P. C. GARFIELD. 1982. Size dependence of growth rate, respiratory electron transport system activity, and chemical composition in marine diatoms in the laboratory. *J. Phycol.* **18**: 58–63.
- BROWN, J. H., G. B. WEST, AND B. J. ENQUIST. 2000. Scaling in biology: patterns and processes, causes and consequences, p. 1–24. *In* J. H. Brown and G. B. West [eds.], *Scaling in biology*. Oxford Univ. Press.
- CAVENDER-BARES, K. K., A. RINALDO, AND S. W. CHISHOLM. 2001. Microbial size spectra from natural and nutrient enriched ecosystems. *Limnol. Oceanogr.* **46**: 778–789.
- CERMEÑO, P., P. ESTÉVEZ-BLANCO, E. MARAÑÓN, AND E. FERNÁNDEZ. 2005a. Maximum photosynthetic efficiency of size-fractionated phytoplankton assessed by ^{14}C -uptake and fast repetition rate fluorometry. *Limnol. Oceanogr.* **50**: 1438–1446.
- , E. MARAÑÓN, D. HARBOUR, AND R. P. HARRIS. 2006. Invariant scaling of phytoplankton abundance and cell size in contrasting marine environments. *Ecol. Lett.* **9**: 1210–1215.
- , ———, J. RODRÍGUEZ, AND E. FERNÁNDEZ. 2005b. Large-sized phytoplankton sustain higher carbon-specific photosynthesis than smaller cells in a coastal eutrophic ecosystem. *Mar. Ecol. Prog. Ser.* **297**: 51–60.
- CHISHOLM, S. W. 1992. Phytoplankton size, p. 213–237. *In* P. G. Falkowski and A. D. Woodhead [eds.], *Primary productivity and biogeochemical cycles in the sea*. Plenum Press.
- CLAUSTRE, H., M. BABIN, D. MERIEN, J. RAS, L. PRIEUR, AND S. DALLOT. 2005. Toward a taxon-specific parameterization of bio-optical models of primary production: A case study in the North Atlantic. *J. Geophys. Res.* **110**: C07S12, doi:10.1029/2004JC002634.
- DAMUTH, J. 1981. Population density and body size in mammals. *Nature* **290**: 699–700.
- ENQUIST, B. J., J. H. BROWN, AND G. B. WEST. 1998. Allometric scaling of plant energetics and population density. *Nature* **395**: 163–165.
- FALKOWSKI, P. G., R. T. BARBER, AND V. SMETACEK. 1998. Biogeochemical controls and feedbacks on ocean primary production. *Science* **281**: 200–281.
- FINKEL, Z. V. 2001. Light absorption and size scaling of light-limited metabolism in marine diatoms. *Limnol. Oceanogr.* **46**: 86–94.
- , A. J. IRWIN, AND O. SCHOFIELD. 2004. Resource limitation alters the $3/4$ size scaling of metabolic rates in phytoplankton. *Mar. Ecol. Prog. Ser.* **273**: 269–279.
- IRIGOIEN, X., K. J. FLYNN, AND R. P. HARRIS. 2005. Phytoplankton blooms: A ‘loophole’ in microzooplankton grazing impact? *J. Plankton Res.* **27**: 313–321.
- JOINT, I. 1991. The allometric determination of pelagic production rates. *J. Plankton Res.* **13**: 69–81.
- JOINT, I. R., AND A. J. POMROY. 1988. Allometric estimation of the productivity of phytoplankton assemblages. *Mar. Ecol. Prog. Ser.* **47**: 161–168.
- KJØRBOE, T. 1993. Turbulence, phytoplankton cell size, and the structure of pelagic food webs. *Adv. Mar. Biol.* **29**: 1–72.
- LATASA, M., X. A. G. MORÁN, R. SCHAREK, AND M. ESTRADA. 2005. Estimating the carbon flux through main phytoplankton groups in the northwestern Mediterranean. *Limnol. Oceanogr.* **50**: 1447–1458.
- LAWS, E. A. 1984. Improved estimates of phytoplankton carbon based on ^{14}C incorporation into chlorophyll *a*. *J. Theor. Biol.* **110**: 425–434.
- LEGENDRE, L., AND F. RASSOULZADEGAN. 1996. Food-web mediated export of biogenic carbon in oceans. *Mar. Ecol. Prog. Ser.* **145**: 179–193.
- LI, W. K. W. 2002. Macroecological patterns of phytoplankton in the north western North Atlantic Ocean. *Nature* **419**: 154–157.
- LÓPEZ-URRUTIA, Á., E. SAN MARTÍN, R. P. HARRIS, AND X. IRIGOIEN. 2006. Scaling the metabolic balance of the oceans. *Proc. Natl. Acad. Sci. U.S.A.* **103**: 8739–8744.
- MARAÑÓN, E., P. M. HOLLIGAN, R. BARCIELA, N. GONZÁLEZ, B. MOURIÑO, M. J. PAZÓ, AND M. VARELA. 2001. Patterns of phytoplankton size-structure and productivity in contrasting open ocean environments. *Mar. Ecol. Prog. Ser.* **216**: 43–56.
- , ———, M. HOLLIGAN, M. VARELA, B. MOURIÑO, AND A. J. BALE. 2000. Basin-scale variability of phytoplankton biomass, production and growth in the Atlantic Ocean. *Deep-Sea Res. I* **47**: 825–857.
- NIKLAS, K. J., AND B. J. ENQUIST. 2001. Invariant size scaling relationships for interspecific plant biomass production rates and body size. *Proc. Natl. Acad. Sci. U.S.A.* **98**: 2922–2927.
- PETERS, R. H. 1983. *The ecological implications of body size*. Cambridge Univ. Press.
- RAVEN, J. A. 1998. Small is beautiful: the picophytoplankton. *Funct. Ecol.* **12**: 503–513.
- REICH, P. B., M. G. TJOELKER, J. L. MACHADO, AND J. OLEKSYN. 2006. Universal scaling of respiratory metabolism, size and nitrogen in plants. *Nature* **439**: 457–461.

- REUL, A., AND OTHERS. 2005. Variability in the spatio-temporal distribution and size-structure of phytoplankton across an upwelling area in the NW-Alboran Sea (W-Mediterranean). *Cont. Shelf Res.* **25**: 589–608.
- RODRÍGUEZ, J., AND OTHERS. 1998. Patterns in the size structure of the phytoplankton community in the deep fluorescence maximum of the Alboran Sea (southwestern Mediterranean). *Deep-Sea Res. I* **45**: 1577–1593.
- , AND OTHERS. 2001. Mesoscale vertical motion and the size structure of phytoplankton in the ocean. *Nature* **410**: 360–363.
- SOMMER, U. 1989. Maximal growth rates of Antarctic phytoplankton: Only weak dependence on cell size. *Limnol. Oceanogr.* **34**: 1109–1112.
- STOLTE, W., T. MCCOLLIN, A. M. NOORDELOOS, AND R. RIEGMAN. 1994. Effect of nitrogen source on the size distribution within marine phytoplankton populations. *J. Exp. Mar. Biol. Ecol.* **184**: 83–97.
- THINGSTAD, T. F., L. ØVREÅS, J. K. EGGE, T. LØVDAL, AND M. HELDAL. 2005. Use of non-limiting substrates to increase size; a generic strategy to simultaneously optimize uptake and minimize predation in pelagic osmotrophs? *Ecol. Lett.* **8**: 675–682.
- ZUBKOV, M. V., M. A. SLEIGH, G. A. TARRAN, P. H. BURKILL, AND J. G. LEAKEY. 1998. Picoplankton community structure on an Atlantic transect from 50°N to 50°S. *Deep-Sea Res. I* **45**: 1339–1355.

Received: 30 November 2006

Accepted: 24 April 2007

Amended: 4 May 2007